

1 Efficient synthesis of rare disaccharides by
2 engineered β -glucosidase based on hydropathy
3 index

4 Kangle Niu[†], Zhengyao Liu[†], Yuhui Feng[†], Tianlong Gao[†], Zhenzhen Wang[†], Piaopiao
5 Zhang[‡], Zhiqiang Du[†], Daming Gao[§], and Xu Fang^{†, ||, *}

6 [†] State Key Laboratory of Microbial Technology, Shandong University, Qingdao
7 266237, China

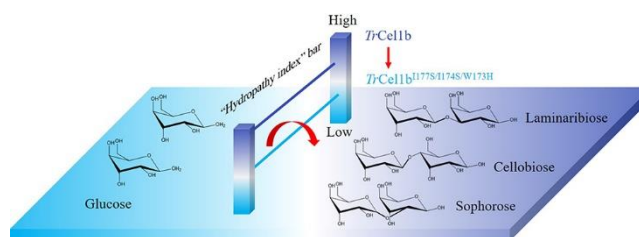
8 [‡] Yantai Huakangrongzan Biotechnology Co., Ltd, Yantai 264006, China.

9 [§] Department of Rehabilitation Science, Graduate School of Health Science, Kobe
10 University, Kobe 6540142, Japan

11 ^{||} National Glycoengineering Research Center, Shandong University, Qingdao
12 266237, China

13

14



15

16 **ABSTRACT:** Oligosaccharides have important therapeutic applications. A useful
 17 route for oligosaccharides synthesis, especially rare disaccharides, is reverse hydrolysis
 18 by β -glucosidase. However, the low conversion efficiency of disaccharides from
 19 monosaccharides limits its large-scale production because the equilibrium is biased in
 20 the direction of hydrolysis. Based on the analysis of the docking results, we
 21 hypothesized that the hydrophathy index of key amino acid residues in the catalytic site
 22 is closely related with disaccharide synthesis and more hydrophilic residues located in
 23 the catalytic site would enhance reverse hydrolysis activity. In this study, positive
 24 variants *TrCel1b*^{I177S}, *TrCel1b*^{I177S/I174S}, and *TrCel1b*^{I177S/I174S/W173H}, and one negative
 25 variant *TrCel1b*^{N240I} were designed according to the Hydrophathy Index For Enzyme
 26 Activity (HIFEA) strategy. The reverse hydrolysis with *TrCel1b*^{I177S/I174S/W173H} was
 27 accelerated and then the maximum total production (195.8 mg/ml/mg enzyme) of the
 28 synthesized disaccharides was increased 3.5-fold compared to that of wildtype. On the
 29 contrary, *TrCel1b*^{N240I} lost reverse hydrolysis activity. The results demonstrate that the
 30 average hydrophathy index of the key amino acid residues in the catalytic site of *TrCel1b*
 31 is an important factor for the synthesis of laminaribiose, sophorose, and cellobiose. The

32 HIFEA strategy provides a new perspective for the rational design of β -glucosidases

33 used for the synthesis of oligosaccharides.

34 **KEYWORDS:** β -glucosidase, hydropathy index, disaccharide synthesis, reverse

35 hydrolysis reaction, site-directed mutagenesis

36

INTRODUCTION

Oligosaccharides are widely distributed in nature and are used in the food and medical industries.¹⁻⁹ Oligosaccharides are mainly prepared by extraction and isolation from a variety of natural plants, by chemical synthesis or biosynthesis.^{1,10,11} Extraction from plants is limited by the source plant and its terrestrial distribution. The biosynthesis of oligosaccharides via enzymatic synthesis technique *in vitro* has recently received increasing attention due to attributes including mild reaction temperature and excellent regio- and stereo-selectivity without the need for masking of functional groups.¹² Enzymatic synthesis of oligosaccharides is mainly catalyzed by glycosidases or glycosyltransferases.¹⁰ Synthesis of oligosaccharides by glycosidases has many advantages that include of simplicity, reliability, ease of operation, and inexpensive donor substrates,^{13,14} compared with catalysis by glycosyltransferases, which requires activation and expensive donor substrates.^{14,15} These facts favor glycosidase as an economically feasible approach in the production of oligosaccharides.¹⁶ Furthermore, some high value-added rare oligosaccharides, such as laminaribiose, gentiobiose, and sophorose, have been produced using glycosidases.^{9,17,18} These oligosaccharides reportedly have potential applications in food and enzyme industries.¹⁹⁻²²

In addition to glycosidic bond cleavage, glycoside hydrolases (GHs) can be used for the synthesis of glycoside bonds *in vitro* via reverse hydrolysis reaction without the need for cofactors, such as uridine diphosphate.^{3,10,16,23,24} Recently, several glycosidases, such as endo- α -N-acetylgalactosaminidase, α -mannosidase, β -galactosidase, and β -glucosidase, have been used to synthesize glycosides via the reverse hydrolysis

59 reaction.³ 4-Butanoic acid-*N*-butyl-amide-1-*O*- β -D-glucopyranoside, 3-butanoic acid
60 ethyl ester-1-*O*- β -D-glucopyranoside, 2-(trimethylsilyl)-ethyl-1-*O*- β -D-
61 glucopyranoside, laminaribiose, sophorose, cellobiose, and gentiobiose have been
62 synthesized by via reverse hydrolysis reaction using β -glucosidase derived from
63 almond.^{17,25} Furthermore, protein engineering of GHs has been widely used to eliminate
64 hydrolytic activity and improve synthetic activity. An important strategy is to disrupt
65 the binding of catalytic water. Honda et al. reported that hydrogen-bonding interaction
66 with catalytic water that reduced the hydrolytic reactivity of an inverting xylanase was
67 dramatically decreased by eliminating the retention of the nucleophilic water molecule
68 at the key amino acid residue.²⁶ Other studies have focused on improving the
69 hydrophobicity of the entrance to the active site^{27,28} or acceptor subsite.²⁹

70 In this study, we report the ability of β -glucosidase *Tr*Cell1b from *Trichoderma reesei*
71 to simultaneously catalyze the synthesis of three disaccharides (laminaribiose,
72 sophorose, and cellobiose) from glucose. The three-dimensional structure of *Tr*Cell1b
73 was obtained by SWISS-MODEL and docked with cellobiose as the model of
74 disaccharides. Based on the analysis of the docking results, we hypothesized that the
75 hydropathy index of key amino acid residues in the catalytic site is closely related with
76 disaccharide synthesis and more hydrophilic residues located in the catalytic site would
77 enhance reverse hydrolysis activity.

78 To verify our deduction, the Hydrophathy Index For Enzyme Activity (HIFEA)
79 strategy was devised. Three hydrophobic amino acid residues in the catalytic site were
80 mutated into hydrophilic residues, which generated the maximal change in the

81 hydropathy index. Three variants were obtained: *TrCel1b*^{I177S}, *TrCel1b*^{I177S/I174S}, and
82 *TrCel1b*^{I177S/I174S/W173H}. Additionally, the variant *TrCel1b*^{N240I} was obtained by
83 improving the hydrophobicity in the catalytic site. The production of synthesized
84 disaccharides by the three variants were investigated. Total production (195.8
85 mg/ml/mg enzyme) of the synthesized disaccharides was increased 3.5 times, compared
86 to that of the wild type. Especially, the production of laminaribiose and sophorose
87 reached 92.3 and 71.1 mg/ml/mg enzyme. The findings indicate the value of the HIFEA
88 strategy in providing a new perspective for the rational design of β -glucosidases used
89 for the synthesis of oligosaccharides.

RESULTS AND DISCUSSION

The rational design of *TrCel1b*. *TrCel1b* (GenBank no. EGR49111.1) in *T. reesei* belongs to the GH1 family and shares 92, 52, 52, 39, and 38% amino acid sequence identity with GH1 family β -glucosidase *ThBgl2* (5JBO), *ThBgl1* (5JBK), *HiBG* (AII80277.1), *NkBgl* (BAB91145.1), and *CaBglA* (JX030398.1), respectively. Mature *TrCel1b* consists of 484 amino acids with a molecular weight of 55.1 kDa. As shown in Fig. S1, β -glucosidases *ThBgl1* and *ThBgl2*, which have a relatively close evolutionary relationship with *TrCel1b*, synthesize oligosaccharides.³⁰ The three-dimensional structure of *TrCel1b* was predicted based on the structure of its variant (PDB ID: 6KHT). The structure shared 100% identity with *TrCel1b* by SWISS-MODEL. A typical TIM-barrel structure of $(\alpha/\beta)_8$ fold was evident in *TrCel1b* (Fig. 2A), as well as the other GH1 family members, such as β -glucosidase *ThBgl2*.

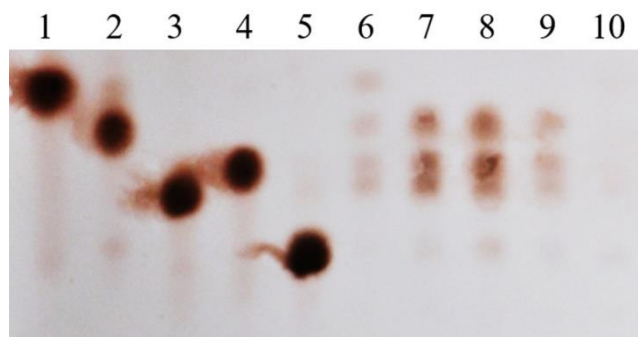
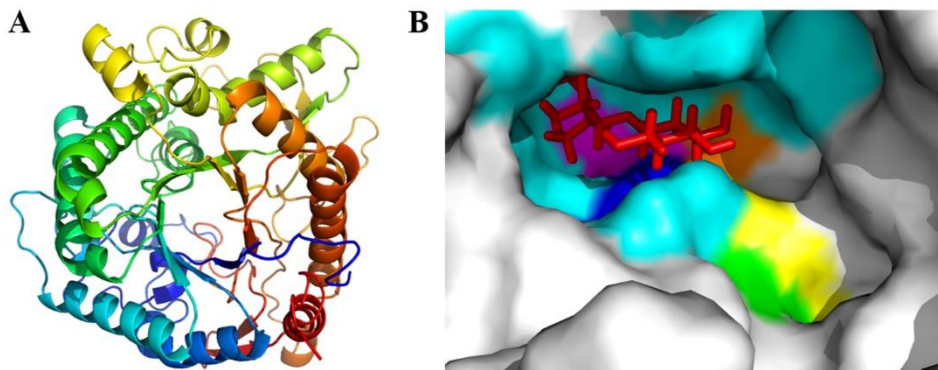


Figure 1. High-performance TLC analysis of products. Lane 1: Glucose; Lane 2: Laminaribiose; Lane 3: Cellobiose; Lane 4: Sophorose; Lane 5: Gentiobiose; Lane 6: Reaction solution synthesized by *TrCel1b*; Lane 7: Reaction solution synthesized by *TrCel1b*^{I177S}; Lane 8: Reaction solution synthesized by *TrCel1b*^{I177S/I174S}; Lane 9: Reaction

108 solution synthesized by *TrCel1b*^{I177S/I174S/W173H}; Lane 10: Reaction solution synthesized by
109 *TrCel1b*^{N240I}.

110 To assess its function, *TrCel1b* was heterologously expressed in *Escherichia coli* was
111 suspended in 4.4 M glucose solution at 30 °C. Laminaribiose, sophorose, and cellobiose
112 were synthesized by the *TrCel1b* suspension based on the result of thin layer
113 chromatography analysis (Fig. 1). The results indicate that the three disaccharides were
114 simultaneously produced though the reverse hydrolysis reaction with inexpensive glucose
115 as the glucosyl donor. Moreover, the production of laminaribiose and sophorose was
116 similar, with the production of cellobiose being markedly lower (Fig. S2 A-L, A-S, A-C).



117
118 Figure 2. Structural-guided rational design of β -glucosidase *TrCel1b*. (A) Homology
119 modeling of the 3-D structure of *TrCel1b* based on the crystal structure of 6KHT. (B) The
120 flexible docking between *TrCel1b* and cellobiose. Cellobiose is depicted in red, the
121 catalytic amino acid residues- E171 and E383 are depicted in magenta, W173, I174, I177
122 and N240 are depicted in yellow, blue, green, and orange, the hydrophilic amino acid
123 residues around cellobiose are depicted in cyan.

124 To improve the production of disaccharides, interaction between *TrCel1b* and cellobiose
125 as the model of disaccharide was predicted with Autodock 1.5.6. The result is presented in

Fig. 2B. The amino acid residues surrounded by the glucose moiety in aglycone subsite (+1 subsite) reportedly has a significant effect on synthesis capacity compared to the residues surrounded by the glucose moiety of cellobiose at the -1 subsite.^{27,29-31} The glucose moiety of cellobiose in the aglycone subsite is surrounded by two hydrophobic residues, W173 and I174, and two hydrophilic residues, Y178 and N240, within a distance of 3.1 Å. The predicted distances between W173, I174, Y178, or N240 and cellobiose were 3.1, 2.8, 2.1, and 2.1 Å, respectively. The extremely hydrophobic residue I177 was also found at the +2 subsite at a distance of 6.4 Å. The hydropathy index of I, W, Y, and N was 4.5, -0.9, -1.3, and -3.5, respectively.

To verify our hypothesis, the HIFEA strategy was applied to improve the reverse hydrolysis activity by reducing the average hydropathy index of key amino acid residues in catalytic site (I_{ah}) of *TrCell1b*. I_{ah} was defined as the sum of the hydropathy index of amino acid residues 173, 174, 177, and 240 divided by their number, namely, $I_{ah} = (I_{h, 173} + I_{h, 174} + I_{h, 177} + I_{h, 240}) / 4$. Three hydrophobic amino acid residues in the catalytic site were mutated into hydrophilic residues and three variants *TrCell1b*^{I177S}, *TrCell1b*^{I177S/I174S}, and *TrCell1b*^{I177S/I174S/W173H} were obtained. Additionally, the variant *TrCell1b*^{N240I} was obtained by improving the hydrophobicity in the catalytic site. The I_{ah} of *TrCell1b* and its variants was calculated according to the hydropathy index.³² The I_{ah} of *TrCell1b*, *TrCell1b*^{I177S}, *TrCell1b*^{I177S/I174S}, *TrCell1b*^{I177S/I174S/W173H}, and *TrCell1b*^{N240I} was 1.15, -0.175, -1.5, -2.075, and 3.15, respectively. The findings revealed that I_{ah} changed along with the mutation. The hydrophobic interaction between these key amino acid residues and disaccharides was weakened when I_{ah} was reduced by the mutation of the hydrophobic residues located in the catalytic site of W173, I174, and/or I177 to the hydrophilic residues,

which facilitated the release of disaccharide. Finally, production of disaccharides synthesized by reverse hydrolysis was improved. On the contrary, reverse hydrolysis was repressed when the hydrophilic residues were mutated into hydrophobic residues.

Identification of products synthesized by *TrCel1b* wildtype and its variants. Purified *TrCel1b*^{I177S}, *TrCel1b*^{I177S/I174S}, *TrCel1b*^{I177S/I174S/W173H}, and *TrCel1b*^{N240I} displayed a similar molecular weight of 74 kDa, compared to the size of *TrCel1b* (Fig. S3), consistent with the molecular weight predicted by the ExPASy website (https://web.expasy.org/compute_pi/). The products synthesized by these variants, except *TrCel1b*^{N240I}, were laminaribiose, sophorose, and cellobiose, respectively (Fig. 1, lane 7–9). The hydrolysis activities of the variants decreased as the I_{ah} of variants decreased (Fig. 3A) and β -glucosidase activity of *TrCel1b*^{I177S/I174S/W173H} was almost lost, compared to 0.35 U/mg soluble protein of *TrCel1b*. However, there was no significant change of β -glucosidase activity between *TrCel1b* and *TrCel1b*^{N240I}. On the contrary, the production of disaccharides was enhanced as the I_{ah} of the variants decreased (Fig. 3B). The disaccharide production of *TrCel1b*^{I177S/I174S/W173H} increased 3.5 times, reaching 195.8 mg/ml/mg enzyme, compared with that of *TrCel1b*. On the contrary, the variant *TrCel1b*^{N240I} with an I_{ah} of 3.15 displayed no disaccharide synthetic activity. As shown in Fig. S2, the disaccharides laminaribiose, sophorose, and cellobiose were synthesized by *TrCel1b*^{I177S}, *TrCel1b*^{I177S/I174S}, and *TrCel1b*^{I177S/I174S/W173H} the same as that of their wildtype protein. Moreover, the production of laminaribiose, sophorose, and cellobiose synthesized by *TrCel1b*^{I177S}, *TrCel1b*^{I177S/I174S}, and *TrCel1b*^{I177S/I174S/W173H} were greater than those of *TrCel1b* (Fig. S2). These results indicated that the decreased I_{ah} of *TrCel1b* was favorite for the reverse hydrolysis reaction.

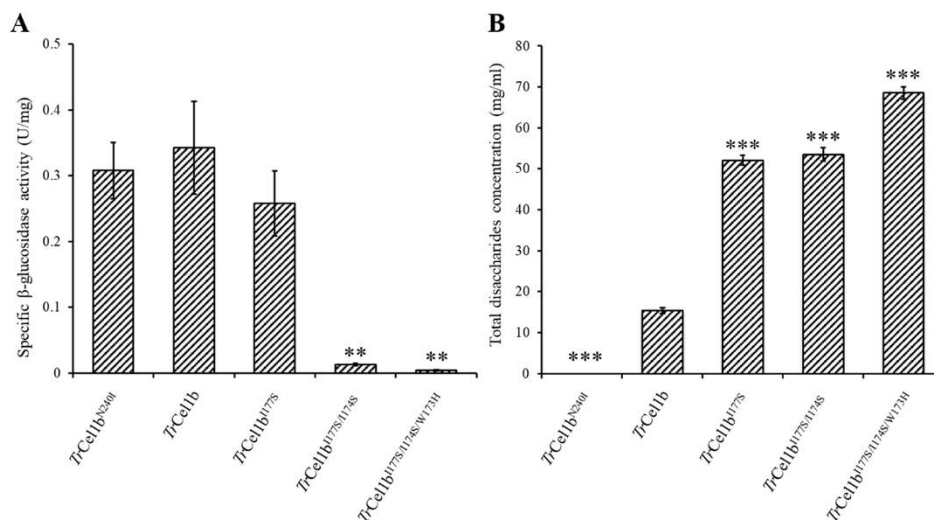


Figure 3. The specific β -glucosidase activity (A) of *TrCell1b* and its variants and the total disaccharides production (B) synthesized by *TrCell1b* and its variants using 80% (w/v) glucose as the substrate for 72 hours. * $p < 0.05$; ** $p < 0.01$; *** $p < 0.001$. The statistically significant difference was performed between *TrCell1b* and its variants.

Glucose was used as the substrate (10, 20, 40, 60, and 80%) for reverse hydrolysis and the laminaribiose, sophorose and cellobiose productions were measured by high-performance liquid chromatography (HPLC) (Fig. S2). The productions of laminaribiose, sophorose, and cellobiose productions were increased with increasing glucose concentration (10–80%), and the productions of laminaribiose and sophorose were increased when the I_{ah} value of the variants was decreased (Fig. S3). Laminaribiose production was the highest among the three disaccharides. The maximal laminaribiose production by *TrCell1b*^{I177S}, *TrCell1b*^{I177S/I174S}, and *TrCell1b*^{I177S/I174S/W173H} reached 57.1, 78.9, 92.3 mg/ml/mg enzyme, and increased 1.8-, 2.8-, and 3.5 -fold, compared to that of *TrCell1b*, respectively. Sophorose production was markedly higher than that of cellobiose, and its maximal productions of *TrCell1b*^{I177S}, *TrCell1b*^{I177S/I174S}, and *TrCell1b*^{I177S/I174S/W173H}

reached 50.9, 56.9, 71.1 mg/ml/mg enzyme, respectively. These results indicated a direct relationship between the reverse hydrolysis activity and the I_{ah} value of *Tr*Cell1b.

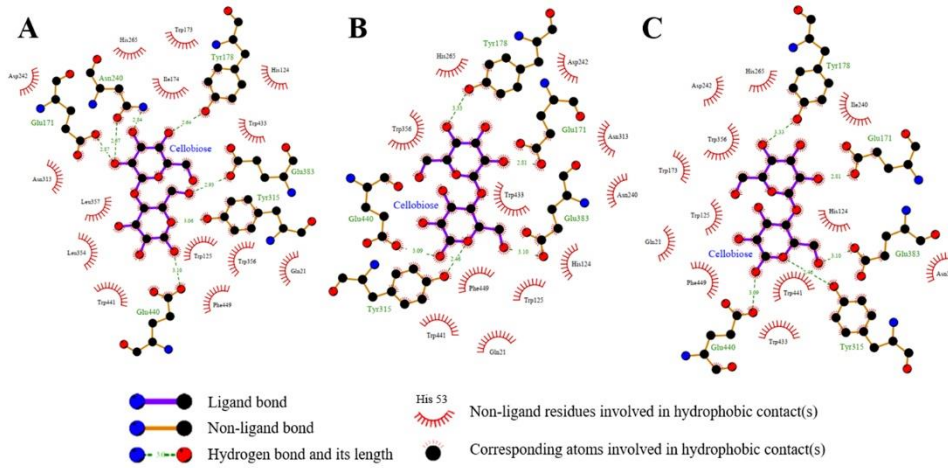


Figure 4. The interaction profiles between *Tr*Cell1b (A), *Tr*Cell1b^{I177S/I174S/W173H} (B) or *Tr*Cell1b^{N240I} (C) and cellobiose analyzed by LigPlot, respectively.

To study the effect of mutation on the interaction between protein and disaccharide, cellobiose was docked with *Tr*Cell1b and its variants using Autodock software and the result of docking was analyzed by LigPlot. The hydrophobic interaction between cellobiose and the amino acid residues of *Tr*Cell1b^{I177S/I174S/W173H} (Fig. 4B) became weak, compared to that of *Tr*Cell1b (Fig. 4A). The number of residues that hydrophobically interacted with cellobiose in *Tr*Cell1b^{I177S/I174S/W173H} and *Tr*Cell1b was 16 and 20, respectively. The hydrophobic interactions between the W173 and I174 residues and cellobiose disappeared since the two residues were mutated into the hydrophilic residues (Fig. 4A and 4B). These results were verified using Discovery studio (Fig. S4).

Compared with *Tr*Cell1b, the I_{ah} of *Tr*Cell1b^{I177S/I174S/W173H} decreased, which was beneficial for the release of the cellobiose product. On the contrary, the I_{ah} of *Tr*Cell1b^{N240I} was enhanced and the synthesis activity of *Tr*Cell1b^{N240I} was completely lost (Fig. 3B)

owing to the mutation of the hydrophilic residue N240 to the hydrophobic residue isoleucine (Fig. 4C). The findings provided an obvious indication of a direct relationship between the I_{ah} value of *TrCell1b* and reverse hydrolysis activity. When the I_{ah} value of *TrCell1b* became negative, the reverse hydrolysis activity was enhanced. On the contrary, when the I_{ah} value of *TrCell1b* increased, the reverse hydrolysis activity was abolished. The findings are consistent with our hypothesis that the hydropathy index of key amino acid residues in the catalytic site is closely related with disaccharide synthesis.

Table 1. Thermodynamic parameters for the reverse hydrolysis from glucose to laminaribiose, cellobiose, and sophorose

Process	$K_{eq} (\times 10^{-3})$	$\Delta_r G'^0$ (kJ/mol)	$\Delta_r G'$ (kJ/mol)
2 Glucose = Laminaribiose + H ₂ O	3.5	14.0 ± 6.0	-44.7 ± 6.0
2 Glucose = Cellobiose + H ₂ O	5.4	12.9 ± 3.7	-45.8 ± 3.7
2 Glucose = Sophorose + H ₂ O	3.4	14.1 ± 5.0	-44.6 ± 5.0

$\Delta_r G'^0$: the change in Gibbs free energy of the chemical reaction in standard 1 M concentrations of substrates and products at pH 7.4 with ionic strength of 0.05 M.

K_{eq} : the equilibrium constant of the chemical reaction in standard 1 M concentrations of substrates and products at pH 7.4 with ionic strength of 0.05 M.

$\Delta_r G'$: the change in Gibbs free energy of the chemical reaction in 4.4 M concentrations of substrate at pH 7.4 with ionic strength of 0.05 M.

In this study, an β -glucosidase *TrCell1b* from *T. ressei* was shown to simultaneously synthesize laminaribiose, sophorose, and cellobiose using a high concentration glucose as substrate. As shown in Table 1, the $\Delta_r G'$ of laminaribiose, sophorose, or cellobiose synthesis is <0 indicating it is realizable that laminaribiose, sophorose, and cellobiose were

produced from glucose by *TrCel1b*. Ravet et al. reported that the disaccharides were produced by β -glucosidase derived from almonds.¹⁷ However, most of these disaccharides were gentiobiose, rather than laminaribiose and sophorose. This was the reason why the equilibrium constant (K_{eq}) of the reaction to synthesize laminaribiose, sophorose, and cellobiose (Table 1) was markedly lower than that of gentiobiose (53.8×10^{-3}). There are few reports on laminaribiose and sophorose synthesis, reflecting their low production. To improve the production of disaccharides synthesized by *TrCel1b*, protein engineering was performed using the HIFEA strategy. The production of laminaribiose, sophorose, and cellobiose synthesized by *TrCel1b*^{I177S/I174S/W173H} was increased 3.5-, 2.6-, and 3.9-fold, respectively, compared to that of *TrCel1b* (Fig. S2). Compared with reported β -glucosidases from different species (Table S1), the maximal productions of laminaribiose and sophorose by *TrCel1b*^{I177S/I174S/W173H} reached 92.3 and 71.1 mg/ml/mg enzyme, respectively, and were higher than the results produced by β -glucosidases from *Aspergillus niger*, *Corynascus* sp., *Penicillium verruculosum*, *T. reesei*,¹⁸ and almond.¹⁷ To our knowledge, this is the highest production of laminaribiose and sophorose simultaneously synthesized by β -glucosidase.

CONCLUSIONS

In summary, β -glucosidase *TrCel1b* from *T. reesei* simultaneously synthesized laminaribiose, sophorose, and cellobiose. Three variants (*TrCel1b*^{I177S}, *TrCel1b*^{I177S/I174S}, and *TrCel1b*^{I177S/I174S/W173H}) with improved disaccharide production were obtained using the HIFEA strategy. The I_{ah} of β -glucosidase *TrCel1b* is an important factor for the production of laminaribiose, sophorose, and cellobiose. The decreased I_{ah} value of *TrCel1b*

improved the synthetic activity and reduced the hydrolytic activity. The HIFEA strategy is implicated as a new avenue for the production of high value-added rare disaccharides.

EXPERIMENTAL SECTION

Chemicals, plasmids, and culture media. Laminaribiose, sophorose, *p*-nitrophenol (*p*NP), and *p*-nitrophenol- β -D-glucoside(*p*NPG) were purchased from Sigma-Aldrich Corporation (St. Louis, MO, USA). Kanamycin and isopropyl-1-thio- β -D-galactopyranoside (IPTG) were purchased from Gen-view Scientific Inc. (El Monte, CA, USA). The KOD-Plus-Mutagenesis Kit was purchased from Toyobo Co., Ltd. (Osaka, Japan). All other chemicals were from Sangon Biotech Co., Ltd. (Shanghai, China). Plasmid pET-32a was purchased from Invitrogen (Carlsbad, CA, USA). Restriction enzymes and T4 DNA ligase were purchased from Thermo Fisher Scientific (Shanghai, China). Primers were synthesized by Sangon Biotech Co., Ltd. *Escherichia coli* DH5 α and *E. coli* BL21 (DE3) was purchased from TransGen Biotech (Beijing, China).

Site-directed mutagenesis. *Tr*Cell1b (GenBank accession number: AAP57758.1) was amplified from the cDNA of *T. reesei* QM6a (ATCC 13631) with primers harboring *Eco*RI and *Hind*III sites, and ligated into pET-32a after it was digested with the same enzymes to obtain the recombinant vector pET-32a-WT. The recombinant vectors pET-32a-I177S, pET-32a-I177S/I174S, pET-32a-I177S/I174S/W173H, and pET-32a-N240I were constructed using the aforementioned KOD-Plus-Mutagenesis Kit. Oligonucleotides used in this study for plasmid constructions are listed in Supplementary Table S2.

Expression and purification. The constructed vectors were introduced into *E. coli* BL21(DE3) for protein expression and transformants were selected on LB plates

containing 10 µg/ml ampicillin as previously described.³³ These proteins were purified from the supernatant with His SpinTrap columns (GE Healthcare, Uppsala, Sweden) as previously described.³⁴ The purified protein of *TrCell1b* and its variants was analyzed by sodium dodecyl sulfate-polyacrylamide gel electrophoresis as previously described.³⁵

Measurement of β -glucosidase activity and enzymatic synthesis of disaccharides. β -glucosidase activity was measured as we previously described, except that the temperature was 30 °C.³⁶ The unit of β -glucosidase activity were defined as the amount of enzyme required to release total reducing sugar equivalent to 1 µmol *p*NP per min. Ten milliliter reaction mixtures, containing 100, 200, 400, 600, or 800 g glucose/l, 500 µl glycerol, and 10 mg sodium nitride in 50 mM phosphate buffer at pH 7.4, were loaded with 3.5 mg of *TrCell1b* and its variants. The reactions were carried out in 50 ml centrifuge tube at 30 °C for 72 h. Three independent replicates were carried out and reaction samples were taken at 0, 2, 4, 6, 8, 10, 19, 24, 34, 48, and 72 h.

The products were analyzed by HPLC as we previously described.³⁷ An Inertsil NH₂ column (250 mm × 7.8 mm; Shimadzu, Kyoto, Japan) and 80% acetonitrile as the mobile phase (1.0 ml/min, 45 °C) were used. Synthesized disaccharides products were detected by TLC following the removal of glucose from the solution. TLC was performed on aluminum-backed sheets of silica gel 60F₂₅₄ (E. Merck) that were 0.2 mm thick. Elution was carried out with *n*-butanol: ethanol: water (5:3:2). The plates were visualized by exposure to staining solution containing 3 g phenol, 5 ml concentrated sulfuric acid and 95 ml alcohol followed by charring. Thermodynamic parameters for the reverse hydrolysis reaction from glucose to laminaribiose, sophorose, and cellobiose at pH 7.4 with an ionic strength of 0.05 M was calculated using the eQuilibrator.³⁸

The phylogenetic and structural analysis. The phylogenetic tree of *TrCell1b* (GenBank accession no. EGR49111.1) from *T. reesei* QM6a, *ThBgl2* (5JBO) from *T. harzianum*, *ThBgl1* (5JBK) from *T. harzianum*, *HiBG* (AII80277.1) from *Humicola insolens*, *NkBgl* (BAB91145.1) from *Neotermes koshunensis* and *CaBglA* (JX030398.1) from *Caldicellulosiruptor* sp. F32 was generated using MEGA. The three-dimensional structures of *TrCell1b*, *TrCell1b*^{I177S}, *TrCell1b*^{I177S/I174S}, *TrCell1b*^{I177S/I174S/W173H}, and *TrCell1b*^{N240I} were predicted using SWISS-MODEL³⁹ with the crystal structure of *TrCell1b*-H13 (PDB ID: 6KHT) as the template. The structures were illustrated using PyMOL software (Delano Scientific, Palo Alto, CA). The interaction between protein and cellobiose was analyzed by LigPlot⁴⁰ and Discovery Studio Software (Accelrys, San Diego, CA, USA).

Statistics. The Student's t-test was performed for significant differences between two groups of data. P<0.05 was considered statistically significant and standard deviations (SD) were calculated at least in triplicate.

ASSOCIATED CONTENT

Supporting Information

Figure S1. The phylogenetic tree of *TrCell1b* and other GH1 family β -glucosidases.

Figure S2. The disaccharides synthesis of β -glucosidase and its variants under different concentrations of glucose.

Figure S3. SDS-PAGE analysis of purification of *TrCell1b* and its variants.

Figure S4. The interaction profiles between *TrCell1b* (A), *TrCell1b*^{I177S/I174SW173H} (B) or *TrCell1b*^{N240I} (C) and cellobiose analyzed by Discovery Studio 4.5, respectively.

Table S1. The comparison of the production of laminaribiose and sophorose synthesized by β -glucosidase from different species.

Table S2. Primers used in this study.

AUTHOR INFORMATION

Corresponding Author

* Corresponding author: fangxu@sdu.edu.cn

Author Contributions

K.N., Z.L., Y.F. and T.G. carried out protein mutagenesis and purification. K.N., Z.W., P.Z., D.G. carried out biochemical assays. K.N., Z.L. and X.F. carried out structural modeling and docking. Z.W. and X.F. conceived of the study. Z.D. and X.F. oversaw experimental and computational work. K.N., Z.D. and X.F. designed experiments and wrote the manuscript. X.F. coordinated the project.

Funding Sources

This work was supported by National Key R&D Program of China (No. 2018YFA090010), Key Technologies R&D Program of Shandong Province (No. 2018GSF121021), the 111 Project (No. B16030), the State Key Laboratory of Microbial Technology Open Projects Fund and National Natural Science Foundation of China (No.31570040 and 31870785).

Notes

Part of the study was authorized by the patent CN 104232606 B.

337 ACKNOWLEDGMENT

338 We thank Ms. Zhifeng Li, Ms. Rui Wang, and Mr. Chengjia Zhang from State Key
339 Laboratory of Microbial Technology for assistance in protein separation and purification.
340 Thanks for Prof. Huifeng Jiang from Tianjin Institute of Industrial Biotechnology, Chinese
341 Academy of Sciences for his contribution during Discovery Studio analyses. Thank for
342 Prof. Luying Xun for revising the manuscript.

343

344 REFERENCES

- 345 (1) Wen, L.; Edmunds, G.; Gibbons, C.; Zhang, J.; Gadi, M. R.; Zhu, H.; Fang, J.; Liu,
346 X.; Kong, Y.; Wang, P. G. Toward automated enzymatic synthesis of oligosaccharides.
347 *Chem. Rev.* **2018**, 118, 8151-8187.
- 348 (2) Driguez, P. A.; Potier, P.; Trouilleux, P. Synthetic oligosaccharides as active
349 pharmaceutical ingredients: lessons learned from the full synthesis of one heparin
350 derivative on a large scale. *Nat. Prod. Rep.* **2014**, 31, 980-989.
- 351 (3) Lu, L.; Liu, Q.; Jin, L.; Yin, Z.; Xu, L.; Xiao, M. Enzymatic synthesis of rhamnose
352 containing chemicals by reverse hydrolysis. *PloS One*, **2015**, 10, e0140531.
- 353 (4) McCranie, E. K.; Bachmann, B. O. Bioactive oligosaccharide natural products. *Nat.*
354 *Prod. Rep.* **2014**, 31, 1026-1042.
- 355 (5) Schmaltz, R. M.; Hanson, S. R.; Wong, C. H. Enzymes in the synthesis of
356 glycoconjugates. *Chem. Rev.* **2011**, 111, 4259-4307.

- 357 (6) Sears, P.; Wong, C. H. Toward automated synthesis of oligosaccharides and
358 glycoproteins. *Science*, **2001**, 291, 2344-2350.
- 359 (7) Seeberger, P. H.; Werz, D. B. Synthesis and medical applications of oligosaccharides.
360 *Nature*, **2007**, 446, 1046.
- 361 (8) Wang, L.; Song, L.; He, X.; Teng, F.; Hu, M.; Tao, Y. Production of isofloridoside
362 from galactose and glycerol using α -galactosidase from *Alicyclobacillus hesperidum*.
363 *Enzyme Microb. Technol.* **2019**, 109480.
- 364 (9) da Silva, A. S. A.; Molina, J. F.; Teixeira, R. S. S.; Gelves, L. G. V.; Bon, E. P.;
365 Ferreira-Leitão, V. S. Synthesis of disaccharides using β -glucosidases from *Aspergillus*
366 *niger*, *A. awamori* and *Prunus dulcis*. *Biotechnol. Lett.* **2017**, 39, 1717-1723.
- 367 (10) Perugino, G.; Trincone, A.; Rossi, M.; Moracci, M. Oligosaccharide synthesis by
368 glycosynthases. *Trends Biotechnol.* **2004**, 22, 31-37.
- 369 (11) Cheng, C. W.; Wu, C. Y.; Hsu, W. L.; Wong, C. H. Programmable One-Pot
370 Synthesis of Oligosaccharides. *Biochemistry* **2019**.
- 371 (12) Moracci, M.; Trincone, A.; Rossi, M. Glycosynthases: new enzymes for
372 oligosaccharide synthesis. *J. Mol. Catal. B-Enzym.* **2001**, 11, 155-163.
- 373 (13) Cobucci-Ponzano, B.; Strazzulli, A.; Rossi, M.; Moracci, M. Glycosynthases in
374 biocatalysis. *Adv. Synth. Catal.* **2011**, 353, 2284-2300.
- 375 (14) Rye, C. S.; Withers, S. G. Glycosidase mechanisms. *Curr. Opin. Chem. Biol.* **2000**,
376 4, 573-580.

- 377 (15) Srisomsap, C.; Subhasitanont, P.; Techasakul, S.; Surarit, R.; Svasti, J. Synthesis of
378 homo-and hetero-oligosaccharides by Thai rosewood β -glucosidase. *Biotechnol. Lett.* **1999**,
379 21, 947-951.
- 380 (16) Van Rantwijk, F.; Woudenberg-van Oosterom, M.; Sheldon, R. A. Glycosidase-
381 catalysed synthesis of alkyl glycosides. *J. Mol. Catal. B-Enzym.* **1999**, 6, 511-532.
- 382 (17) Ravet, C.; Thomas, D.; Legoy, M. D. Gluco-oligosaccharide synthesis by free and
383 immobilized β -glucosidase. *Biotechnol. Bioeng.* **1993**, 42, 303-308.
- 384 (18) Semenova, M. V.; Okunev, O. N.; Gusakov, A. V.; Sinitsyn, A. P. Disaccharide
385 synthesis by enzymatic condensation of glucose: glycoside linkage patterns for different
386 fungal species. *Open Glycosci.* **2009**, 2, 20-24.
- 387 (19) Sanz, M. L.; Gibson, G. R.; Rastall, R. A. Influence of disaccharide structure on
388 prebiotic selectivity in vitro. *J. Agric. Food Chem.* **2005**, 53, 5192-5199.
- 389 (20) Kurasawa, T.; Yachi, M.; Suto, M.; Kamagata, Y.; Takao, S.; Tomita, F. Induction
390 of cellulase by gentiobiose and its sulfur-containing analog in *Penicillium purpurogenum*.
391 *Appl. Environ. Microbiol.* **1992**, 58, 106-110.
- 392 (21) Loewenberg, J. R.; Chapman, C. M. Sophorose metabolism and cellulase induction
393 in *Trichoderma*. *Arch. Microbiol.* **1977**, 113, 61-64.
- 394 (22) Bucke, C. Review Oligosaccharide Synthesis Using Glycosidases. *J. Chem. Tech.*
395 *Biotechnol.* **1996**, 67, 217-220.

- 396 (23) Rosengren, A.; Butler, S. J.; Arcos-Hernandez, M.; Bergquist, K. E.; Jannasch, P.;
397 Stålbrand, H. Enzymatic synthesis and polymerisation of β -mannosyl acrylates produced
398 from renewable hemicellulosic glycans. *Green Chem.* **2019**, 21, 2104-2118
- 399 (24) Xu, L.; Liu, X.; Yin, Z.; Liu, Q.; Lu, L.; Xiao, M. Site-directed mutagenesis of α -l-
400 rhamnosidase from *Alternaria* sp. L1 to enhance synthesis yield of reverse hydrolysis based
401 on rational design. *Appl. Microbiol. Biotechnol.* **2016**, 100, 10385-10394.
- 402 (25) Fischer, L.; Bromann, R.; Wagner, F. Enantioselective synthesis of several 1-O- β -
403 D-glucoconjugates using almond β -glucosidase (EC 3.2. 1.21). *Biotechnol. Lett.* **1995**, 17,
404 1169-1174.
- 405 (26) Honda, Y.; Fushinobu, S.; Hidaka, M.; Wakagi, T.; Shoun, H.; Taniguchi, H.;
406 Kitaoka, M. Alternative strategy for converting an inverting glycoside hydrolase into a
407 glycosynthase. *Glycobiology* **2008**, 18, 325-330.
- 408 (27) Frutuoso, M. A.; Marana, S. R. A single amino acid residue determines the ratio of
409 hydrolysis to transglycosylation catalyzed by β -glucosidases. *Protein Pept. Lett.* **2013**, 20,
410 102-106.
- 411 (28) Kuriki, T.; Kaneko, H.; Yanase, M.; Takata, H.; Shimada, J.; Handa, S.; Takada, T.;
412 Umeyama, H.; Okada, S. Controlling substrate preference and transglycosylation activity
413 of neopullulanase by manipulating steric constraint and hydrophobicity in active center. *J.*
414 *Biol. Chem.* **1996**, 271, 17321-17329.

- 415 (29) Lundemo, P.; Adlercreutz, P.; Karlsson, E. N. Improved transferase/hydrolase ratio
416 through rational design of a family 1 β -glucosidase from *Thermotoga neapolitana*. *Appl.*
417 *Environ. Microbiol.* **2013**, 79, 3400-3405.
- 418 (30) Florindo, R. N.; Souza, V. P.; Mutti, H. S.; Camilo, C.; Manzone, L. R.; Marana, S.
419 R.; Polikarpov, I.; Nascimento, A. S. Structural insights into β -glucosidase
420 transglycosylation based on biochemical, structural and computational analysis of two
421 GH1 enzymes from *Trichoderma harzianum*. *New Biotechnol.* **2018**, 40, 218-227.
- 422 (31) Lundemo, P.; Karlsson, E. N.; Adlercreutz, P. Eliminating hydrolytic activity
423 without affecting the transglycosylation of a GH1 β -glucosidase. *Appl. Microbiol.*
424 *Biotechnol.* **2017**, 101, 1121-1131.
- 425 (32) Kyte, J.; Doolittle, R. F. A simple method for displaying the hydropathic character
426 of a protein. *J. Mol. Biol.* **1982**, 157, 105-132.
- 427 (33) Xin, Y.; Liu, H.; Cui, F.; Liu, H.; Xun, L. Recombinant *Escherichia coli* with sulfide:
428 quinone oxidoreductase and persulfide dioxygenase rapidly oxidises sulfide to sulfite and
429 thiosulfate via a new pathway. *Environ. Microbiol.* **2016**, 18, 5123-5136.
- 430 (34) Hou, N.; Yan, Z.; Fan, K.; Li, H.; Zhao, R.; Xia, Y.; Xun, L.; Liu, H. OxyR senses
431 sulfane sulfur and activates the genes for its removal in *Escherichia coli*. *Redox Biol.* **2019**,
432 26, 101293.
- 433 (35) Schgger, H. Tricine-sds-page. *Nat. Protoc.* **2006**, 1, 16.

- 434 (36) Liu, K.; Dong, Y.; Wang, F.; Jiang, B.; Wang, M.; Fang, X. Regulation of cellulase
435 expression, sporulation, and morphogenesis by velvet family proteins in *Trichoderma*
436 *reesei*. *Appl. Microbiol. Biotechnol.* **2016**, 100, 769-779.
- 437 (37) Guo, W.; Huang, Q.; Liu, H.; Hou, S.; Niu, S.; Jiang, Y.; Bao, X.; Shen, Y.; Fang,
438 X. *Front. Rational engineering of chorismate-related pathways in Saccharomyces*
439 *cerevisiae* for improving tyrosol production. *Bioeng. Biotech.* **2019**, 7, 152.
- 440 (38) Noor, E.; Haraldsdóttir, H. S.; Milo, R.; Fleming, R. M. T. Consistent estimation of
441 Gibbs energy using component contributions. *PLoS Comput. Biol.* **2013**, 9, e1003098.
- 442 (39) Waterhouse, A.; Bertoni, M.; Bienert, S.; Studer, G.; Tauriello, G.; Gumienny, R.;
443 Heer, F. T.; de Beer, T. A. P.; Rempfer, C.; Bordoli, L.; Lepore, R.; Schwede, T. SWISS-
444 MODEL: homology modelling of protein structures and complexes. *Nucleic Acids Res.*
445 **2018**, 46, W296-W303.
- 446 (40) Wallace, A. C.; Laskowski, R. A.; Thornton, J. M. LIGPLOT: a program to generate
447 schematic diagrams of protein-ligand interaction. *Protein Eng. Des. Sel.* **1995**, 8, 127-134.